frontiers | Frontiers in Marine Science

TYPE Original Research
PUBLISHED 08 January 2024
DOI 10.3389/fmars.2023.1260058

OPEN ACCESS

EDITED BY
Naresh Krishna Vissa,
National Institute of Technology Rourkela, India

REVIEWED BY
Venkata Sai Gulakaram,
Indian National Centre for Ocean Information Services, India
Konda Gopi Nadh,
Indian Institute of Tropical Meteorology, India

*CORRESPONDENCE
Ibrahim Hoteit
ibrahim.hoteit@kaust.edu.sa

RECEIVED 17 July 2023
ACCEPTED 29 November 2023
PUBLISHED 08 January 2024

CITATION
Vasou P, Krokos G, Langodan S, Sofianos S and Hoteit I (2024) Contribution of surface and lateral forcing to the Arabian Gulf warming trend. *Front. Mar. Sci.* 10:1260058. doi: 10.3389/fmars.2023.1260058

Contribution of surface and lateral forcing to the Arabian Gulf warming trend

Panagiotis Vasou[1], George Krokos[2], Sabique Langodan[1,3], Sarantis Sofianos[4] and Ibrahim Hoteit[1]*

[1]Earth Science and Engineering Department, King Abdullah University of Science and Technology (KAUST), Thuwal, Saudi Arabia, [2]Institute of Oceanography, Hellenic Centre for Marine Research, Anavyssos, Greece, [3]Environmental Protection Department, Saudi Aramco, Dhahran, Saudi Arabia, [4]Environmental Physics Division, National and Kapodistrian University of Athens, Athens, Greece

The contribution of surface and lateral forcing to the observed Arabian Gulf warming trend is studied based on the results of a high-resolution (1/100°, 60 vertical layers) MIT general circulation model (MITgcm) covering the period 1993–2021. The model validation against available observations reveals that the simulation satisfactorily reproduces the main features of the Arabian Gulf's dynamics and their variability. We show that the heat content of the Arabian Gulf generally follows the reported variability of sea surface temperature, with significant increasing trends of 0.1×10^7 J m^{-3} and 0.2°C per decade. The interannual variability of the heat content is dominated by the surface heat fluxes, while the long-term warming of the basin is primarily driven by lateral fluxes. The analyses of the heat exchanges through the Strait of Hormuz indicate a pronounced upward trend in the transported heat toward the Arabian Gulf, which is associated with an increase in both the volume and temperature of the exchanged waters. Considering the inflow and outflow in the Strait separately, the temperature increase is more prominent in the inflowing waters; however, the dominant factor driving the rising trend in heat content exchanges is the increase in the volume of waters being exchanged. This implies that the observed warming of the Arabian Gulf during the investigated period is directly related to the acceleration of its overturning circulation.

KEYWORDS

Arabian Gulf, warming trends, heat content, heat budget, interannual variability, surface and lateral fluxes, ocean modeling

1 Introduction

Climate change has continued to intensify over the last decades and global warming has accelerated in a way that has a considerable impact on local weather and climate and ultimately affected local ecosystems and human society (IPCC, 2019). Two of the most important ocean indicators for climate change and global warming rates are the sea surface temperature (SST) and the ocean heat content (OHC) (Garcia-Soto et al., 2021). Several

studies have indicated that during the past decades, the SST has been increasing in the World Ocean and individual ocean basins (Ting et al., 2009; Large and Yeager, 2012; Reid and Beaugrand, 2012; Krokos et al., 2019; Noori et al., 2019; Hereher, 2020; Pisano et al., 2020; Garcia-Soto et al., 2021; Al Senafi, 2022) and that the same has been happening for the OHC (Levitus et al., 2000; Willis et al., 2004; Nagamani et al., 2016; Nath et al., 2016; Cheng et al., 2017; Storto et al., 2019). Belkin (2009) performed a study on large marine ecosystems and suggested a rapid warming rate for the period 1982–2006, which was stronger in small marginal seas. Semi-enclosed basins, in comparison to larger ocean basins, exhibit higher sensitivity to global warming due to their smaller volume and slower water renewal rates (Belkin, 2009; Krokos et al., 2019).

The Arabian Gulf (or simply the Gulf) is a shallow, semi-enclosed basin located between the Arabian Peninsula and southwestern Iran with a length of ~990 km and a width ranging from a minimum of 56 km to a maximum of 340 km (K. O. Emery (2), 1956). It is connected to the Gulf of Oman and the Arabian Sea through the Strait of Hormuz (SoH) (Figure 1). The Gulf has an asymmetric bathymetry, with extended shallow banks in its north and southwestern regions and a trough that extends from the SoH area toward the northern parts of the Gulf along the Iranian coast. While the average depth of the Gulf is only about 35 m, with a maximum at the SoH reaching 110 m, the bottom falls rapidly to more than 2000 m in the Gulf of Oman.

The Arabian Gulf and Gulf of Oman are important basins from an environmental, commercial, industrial, social, and political perspective. In particular, understanding the thermodynamics and circulation dynamics of the Gulf is crucial as it has a considerable influence on various environmental aspects. The environment of the Gulf experiences physical extremes with semi-annual temperature variations exceeding 20°C (Vaughan and Burt, 2016) and salinity values averaging 42 ppt and exceeding 50 ppt in the southern areas (John et al., 1990). Changes in such an extreme environment may have harmful effects on the Gulf marine communities (Bauman et al., 2013).

The thermohaline characteristics of the Gulf are driven by local atmospheric forcing and water exchanges with the open ocean (Al Azhar et al., 2016). The commonly accepted description of water circulation in the Gulf was presented by Michael Reynolds (1993), who incorporated all available observations to date, including those of Emery (1956); Brewer et al. (1978), and Brewer and Dyrssen (1985). Relatively fresher water from the Arabian Sea mainly flows from the northern part of the SoH and drifts toward the southern Iranian coast. A general cyclonic circulation over the entire Gulf drives this water to the northwest and eventually to the southeast shallow region of the Gulf, where it is transformed due to dense water formation. It then sinks and is eventually exported through the southern deep part of the SoH.

Despite the fact that the Gulf is located in the subtropical region, its climate changes from subtropical to tropical during summer due to the dominant arid environment. Estimates for the net surface heat flux over the Gulf vary from an annual mean of 21 Wm^{-2} heat loss to 66 Wm^{-2} heat gain (Hastenrath et al., 1979; Ahmad and Sultan, 1991; Prasad et al., 2001; Johns et al., 2003; Abualnaja, 2009). Evaporation in the Gulf is considerably greater than precipitation. Estimates of evaporation remains largely uncertain, ranging from 1.4 to 5.0 m yr^{-1} (Privett, 1959; Ross and Stoffers, 1978; Meshal and Hassan, 1986; Johns et al., 2003), while precipitation is of the order of 0.07 m yr^{-1} (Michael Reynolds, 1993) to 0.15 m yr^{-1} (Johns et al., 2003). The large annual evaporation over the basin plays a major role in forcing the water exchanges through the SoH. It drives low-salinity Indian Ocean surface water (IOSW) into the Gulf, primarily through the northern part of the SoH (Brewer et al., 1978; Hunter, 1982; Michael Reynolds, 1993; Johns et al., 2003; Vasou et al., 2020), and hypersaline Arabian Gulf water (also known as Persian Gulf

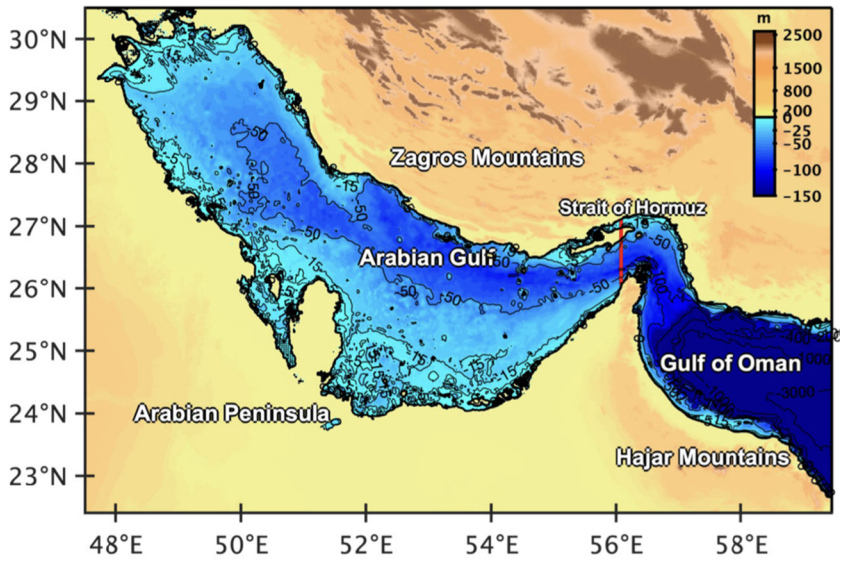

FIGURE 1
Bathymetric map of the model domain covering the Arabian Gulf and the Gulf of Oman. The red line indicates the Strait of Hormuz.

water) exiting to the Gulf of Oman through the deeper southern part of the SoH (Shenn-Yu et al., 1992; Johns et al., 2003; Vasou et al., 2020).

Due to the shallow nature of the Gulf, the SST and the heat balance of the basin are considerably impacted by the atmospheric and advective (through the SoH) forcing (Xue and Eltahir, 2015). Furthermore, the Gulf SST is strongly influenced by the surface fluxes (Xue and Eltahir, 2015). Heat content can alter the sea level due to thermal expansion of the ocean volume (Antonov et al., 2005) and can also influence the SST. Compared to SST, the heat content is a more suitable parameter for examining the warming rate of the basin. It can provide a better understanding for the entire water column in terms of stored heat and its long-term variations. Furthermore, the heat content change (HCC) along with the components defining it, that is, the lateral and surface heat fluxes, provide the means of evaluating the interannual variations and trend of the Gulf warming, while attributing the relative contribution of each forcing.

Because of the sparsity of observations and considerably vague estimates of freshwater and surface and lateral heat fluxes, estimates of the Gulf's heat and water budgets as well as its heat content remain largely uncertain. Several regional modeling studies have been conducted to simulate and study the hydrodynamics of the Gulf. Most of these studies investigated the general circulation in the basin (Shenn-Yu et al., 1992; Sadrinasab and Kämpf, 2004; Kämpf and Sadrinasab, 2006; Yao and Johns, 2010a; Yao and Johns, 2010b; Hassanzadeh et al., 2011; Hosseinibalam et al., 2011; Pous et al., 2015; Al Azhar et al., 2016; Alosairi and Pokavanich, 2017; Layeghi et al., 2019; Al-Shehhi et al., 2021), while others examined the basin's response to winds (Thoppil and Hogan, 2010b; Hassanzadeh et al., 2011; Hosseinibalam et al., 2011; Pous et al., 2013b). Certain studies explored the role of tides (Azam et al., 2006; Pous et al., 2013a) and mesoscale processes (Thoppil and Hogan, 2010a), and others the heat, salinity, and freshwater budgets (Xue and Eltahir, 2015; Campos et al., 2020). Some of the studies also focused on the water exchanges with the open Ocean through the strait of Hormuz (Thoppil and Hogan, 2009; Lorenz et al., 2020; Vasou et al., 2020). Only a few studies have evaluated the heat budget and its terms in the Gulf, mainly focusing on seasonal time scales, or covered relatively short time periods (Johns et al., 2003; Pous et al., 2015; Xue and Eltahir, 2015; Alsayed et al., 2023). A detailed description of the heat budget and the parameters defining it in terms of interannual variability and trends is still lacking.

Herein, we analyze the results of a regional MIT general circulation model (MITgcm; Marshall et al., 1997) configuration for the Gulf to investigate its long-term variability and trends of SST and OHC. Subsequently, we evaluate the interannual variations of the heat budget terms and the relative contribution of surface and lateral heat fluxes to the Gulf HCC and warming trend. Finally, we examine the variability and trends of the heat content exchanges between the Gulf and the open ocean. Our paper is organized as follows. Section 2 describes the model setup, and validation against satellite-available and *in situ* observations. The trends and interannual variability of SST and heat content are presented in Section 3; in this section we also examine the relative contribution of lateral and surface forcing to the heat content change, and we further investigate the relative role of volume and temperature of the exchanged flow through SoH in impacting the heat exchanges there. Section 4 concludes the study with discussing the main findings and future work.

2 Model description and experimental setup

A regional hydrodynamic simulation for the Gulf was generated using the MITgcm. The basic principles and technical characteristics of this model are thoroughly described in Adcroft et al. (2017). The MITgcm is based on the primitive Navier–Stokes equations on a spherical coordinate under the Boussinesq approximation (Marshall et al., 1997) and is configured here in hydrostatic mode with an implicit free surface. The regional Gulf model domain included the Arabian Gulf and a large part of the Gulf of Oman. The bathymetry is derived from the ETOPO1 global product (NOAA National Geophysical Data Center, 2009). An open boundary is set at ~59.5°E and the model was forced at the boundary with temperature, salinity, sea surface level, and velocity conditions extracted from GLORYS2 (version 4) — the most recent ocean reanalysis product by Mercator Ocean (http://marine.copernicus.eu/). The model has a horizontal grid spacing of ~1 km (1/100°) and 60 vertical, nonuniformly spaced z-layers, with 41 layers covering the first 120 m (0.5 m at the surface, increasing exponentially with depth). The model was forced with atmospheric fields of 5-km horizontal resolution generated by downscaling the ERA-Interim reanalysis (Dee et al., 2011) using the advanced research version of the weather research and forecasting (WRF) model, assimilating all available satellite and conventional observations in the region (Hoteit et al., 2021). It is important to note that the generation of these atmospheric fields was conducted independently of our study and is extensively described in Viswanadhapalli et al. (2017) and Dasari et al. (2022). Furthermore, comprehensive validations of these fields against available observations have been conducted and presented in Langodan et al. (2017) and Viswanadhapalli et al. (2017). These results demonstrated that the regional atmospheric fields substantially improved the representation of regional atmospheric features compared to the original ECMWF fields. These atmospheric fields are available every hour, which was important to account for the diurnal variability of atmospheric variables, particularly near the coastal regions. The atmospheric flux components were estimated using the formulas and coefficients given in Large and Pond (1981). Riverine fluxes are imposed as surface freshwater flux. Four main rivers — the Shatt-Al-Arab, Mand, Hendijan, and Hilleh — are considered following a monthly climatology of their discharge values and temperature, as suggested by Alosairi and Pokavanich (2017).

The Gulf MITgcm configuration was implemented with a third-order, nonlinear, direct space–time flux limited scheme for the

temperature and salinity advection with constant diffusion and viscosity. A Laplacian operator with a diffusion coefficient of 1.2×10^{-5} m^2 s^{-1} was used in the vertical. Unresolved upper ocean mixing processes were parameterized using the K-profile parameterization (KPP; Large et al., 1994). A no-slip condition was applied at the bottom with a quadratic drag coefficient of 2.1×10^{-3}.

The model was initialized from a state of no-motion using annual mean temperature and salinity from the World Ocean Atlas 2018 (WOA18). After a 4-year spin-up run using the 1993 atmospheric forcing and boundary conditions, the model simulation was forced with the downscaled WRF fields for the years 1993–2021.

3 Results

3.1 Model assessment

We started by analyzing the water exchange between the Gulf and the Indian Ocean through the SoH, which serves as representative of the thermohaline-driven overturning circulation. Following that, we assessed the model SST as an indicator of the model response to atmospheric forcing. Additional model validation results can be found in the Supplementary Material, which includes a comparison with available observations of potential temperature and salinity in the water column. The outcomes of this comparison exercise indicate a strong agreement between the model and the observations regarding the variability of the thermohaline properties in the Gulf. The results further suggest a qualitative consistency in the representation of the circulation patterns.

For the evaluation of the exchanges at the SoH, the model outputs were directly compared with available *in situ* measurements of salinity, temperature, and current profiles at the southern part of the SoH, which are available for the period of December 1996 to March 1998 (Johns et al., 2003).

The model is able to reproduce the thermohaline structure and the temporal variability of the exchanges through the SoH, as described by the observations (Figure 2). Near-surface low-salinity values during late winter to spring (February-May; Figure 2 upper panel) are typical of the IOSW inflow, while the deep outflow of high-salinity values during winter (December - March) is representative of dense water formed in the southern banks of the Gulf (Kämpf and Sadrinasab, 2006; Yao and Johns, 2010a; Yao and Johns, 2010b; Pous et al., 2015; Al Azhar et al., 2016). During summer and fall (July to November), the deep outflow, which originates from the northern Gulf (Swift and Bower, 2003; Yao and Johns, 2010b; Pous et al., 2015; Al-Shehhi et al., 2021), is slightly "fresher" than during winter, while the near surface and intermediate flow is more saline during this period. The latter indicates the mixing of dense water coming from the south with fresher water coming from the Gulf of Oman, which eventually outflows through the SoH. The structure of the temperature profiles at the SoH (Figure 2 lower panel) matches and completes the previous descriptions, further revealing the intense cooling with reduced stratification during winter and spring (December to March) and the warm core in the upper ocean layers associated with the well stratified thermocline during summer and fall (July to November) (Swift and Bower, 2003; Kämpf and Sadrinasab, 2006; Yao and Johns, 2010b; Al Azhar et al., 2016).

The along-SoH velocity implies high seasonal variability for the inflow/outflow at the SoH (Figure 3), and is generally consistent

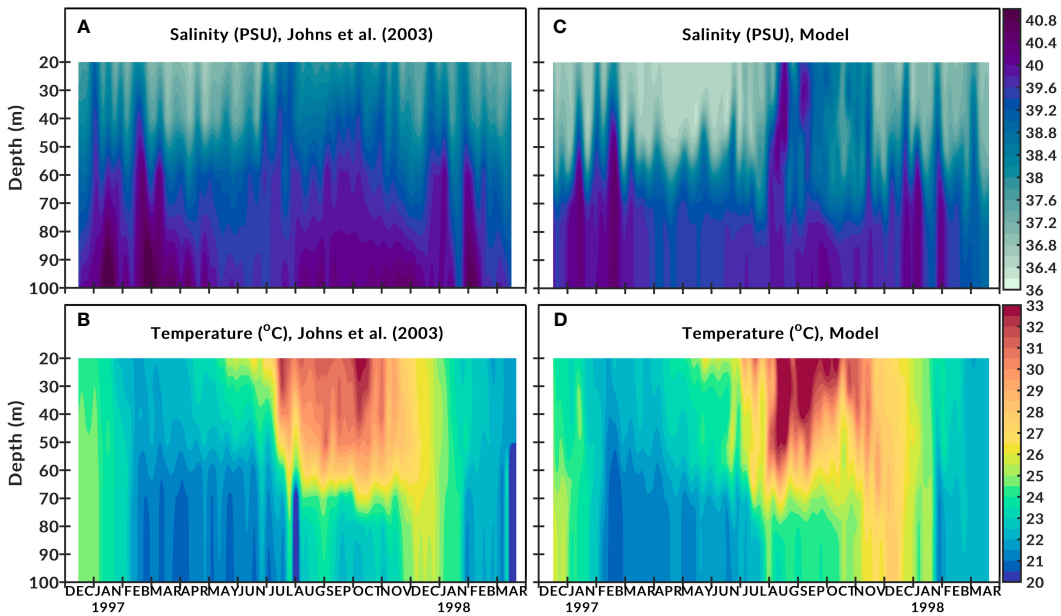

FIGURE 2
Hovmöller diagrams of the observations of Johns et al. (2003) on **(A)** salinity and **(B)** temperature in the Strait of Hormuz and model **(C)** salinity and **(D)** temperature. A low-pass filter of 10 days is applied. The model data span the period from December 1997 to March 1998 in the SoH close to the mooring site of Johns et al. (2003).

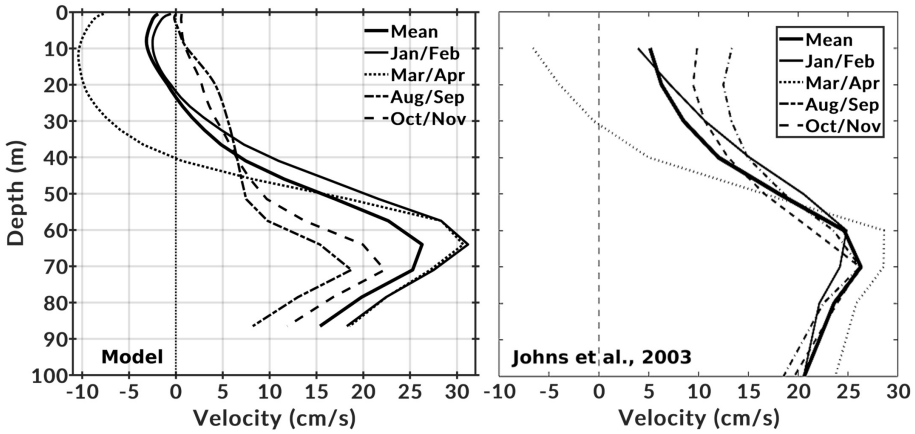

FIGURE 3
Four bimonthly averages and the annual mean of velocity (cm/s) for the year 1997 in the Strait of Hormuz close to the mooring site of Johns et al. (2003) (left panel) and for the observations, as adopted from Johns et al. (2003) (right panel).

with estimates from previous studies based on modeling and observations (Johns et al., 2003; Thoppil and Hogan, 2009; Yao and Johns, 2010b; Hosseinibalam et al., 2011; Pous et al., 2015; Al Azhar et al., 2016; Campos et al., 2020; Vasou et al., 2020). The net transport and deep outflow through the SoH are evaluated at ~0.23 ± 0.01 and ~0.15 ± 0.01 Sv, respectively, similar to estimates based on *in situ* measurements (Table 1). This presented a considerable improvement compared to earlier modeling studies (Yao and Johns, 2010b; Hosseinibalam et al., 2011; Pous et al., 2015; Campos et al., 2020).

The model SST was evaluated against remotely sensed data from the operational SST and sea ice analysis (OSTIA) dataset provided by the UK Met Office (Donlon et al., 2012). The results demonstrate a very good agreement between the model and satellite-derived SSTs in time (Figure 4) and space (Figure 5). The model SST effectively captures the daily and interannual variability throughout the simulation period (Figure 4). Root-mean-squared differences (RMSD) between the daily averaged model and satellite SST within the modeled region are 0.76 ± 0.26°C in winter and 0.85 ± 0.25°C in summer. The spatially averaged correlation coefficients between the model and data daily SST fields are 0.97 ± 0.02 in winter and 0.96 ± 0.04 in summer. The RMSD remains below 1°C across most of the Gulf (Figure 5 upper panel), with a small increase in the northeast during winter (Figure 5B) when surface flux variability is highest, mainly due to strong Shamal winds (Al Senafi and Anis, 2015). The correlation coefficient is spatially uniform and consistently exceeds 0.95 in the majority of the Gulf (Figure 5 lower panel). Comparison of SST trends reveal a close agreement between model and satellite derived data, both temporally and spatially. Average trends across the entire Gulf indicate an increasing trend of 0.2°C per decade in the model results and 0.27°C per decade in the satellite derived SST (Figure 4B). Spatial estimates of SST warming trends in the Gulf ranges from 0.08°C per decade to 0.35°C per decade, with higher values observed in the central and northern regions (Figure S1, Supplementary Material).

The model's ability to accurately represent the Gulf's thermohaline properties and circulation is evident from the overall agreement observed. There is consistency between the model and satellite-derived SST, as well as concurrence in the water exchanges through the SoH and the thermohaline characteristics throughout the water column. This indicates that the model captures the essential dynamics of the Gulf's circulation. The spatial and temporal distribution exhibited by the model's SST aligns well with satellite observations, providing further credibility to the model's reliability. Additionally, the agreement in the flow exchanges through the SoH and the vertical thermohaline properties further supports the model's ability to accurately represent the Gulf's circulation and dynamics throughout the simulation period.

TABLE 1 Comparison of transport estimates through the Strait of Hormuz between the model and that estimated from observations by Johns et al. (2003).

	Inflow (Sv)	Deep outflow (Sv)	Surface outflow (Sv)
Observed	0.233 ± 0.04	0.15 ± 0.03	0.06 ± 0.02
Model	0.2327 ± 0.01	0.148 ± 0.01	0.054 ± 0.01

3.2 Variability and trend of ocean heat content

The simulation results revealed that the basin average SST (Figure 6, black curve) exhibited strong interannual variations with a statistically significant at the 95% confidence level increasing trend of ~0.2°C per decade. Other studies also indicated a general positive trend (Shirvani et al., 2015; Noori et al., 2019; Hereher, 2020; Mogaddam et al., 2020; Al Senafi, 2022) that varied depending on the period as well as the area examined.

All the above-mentioned studies that investigated the response of the Gulf to recent climate variability focus on SST to assess the

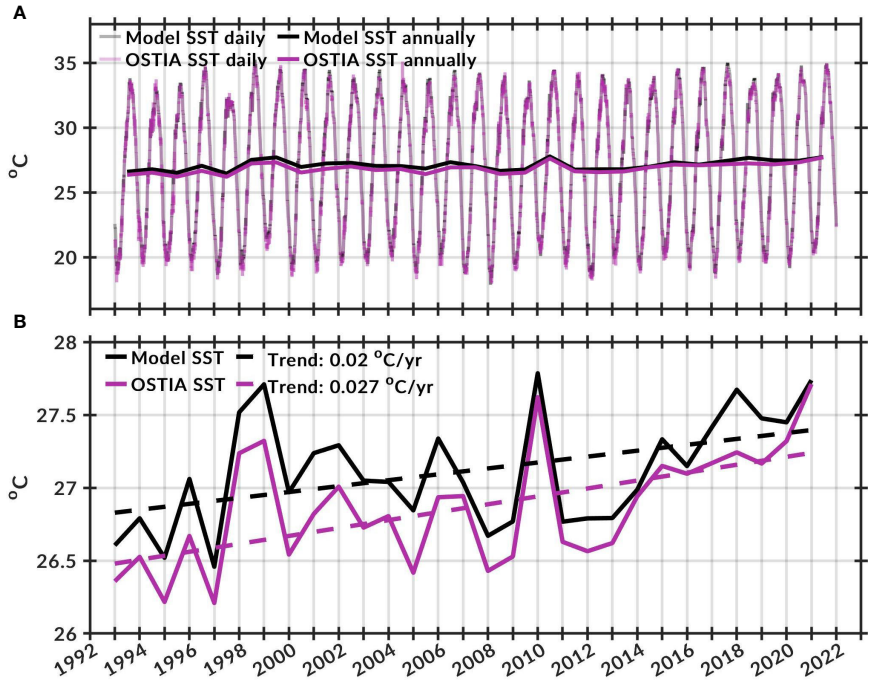

FIGURE 4
Comparisons of the SST averaged over the Gulf, between the model simulation (black lines) and satellite OSTIA data (magenta lines). The solid thick lines represent the annual average values, while faint lines in **(A)** represent the daily values and dashed lines in **(B)** represent the linear trends.

warming rate of the basin. However, the Gulf dynamics are governed by complex processes due to its intricate topography, a three-dimensional exchange flow pattern at the SoH, and dense water formation driving its overturning circulation. Thus, the SST cannot provide a complete representation of the conditions prevailing in the entire water column, particularly in terms of heat storage and interannual variability. To address this, following Meyssignac et al. (2019), we computed the annual mean OHC over

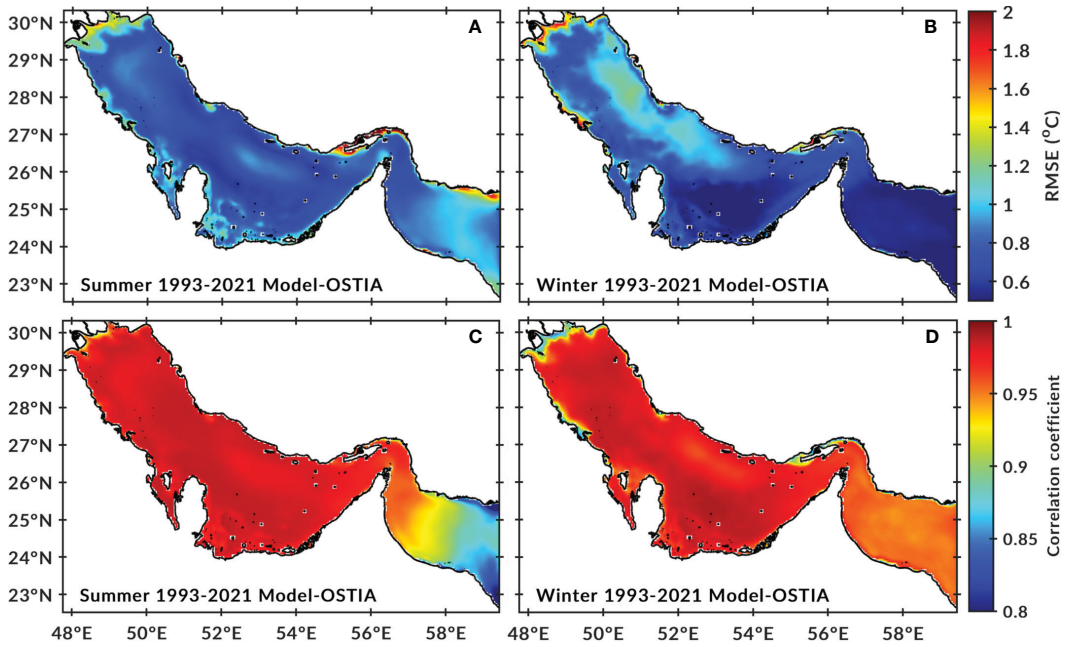

FIGURE 5
(Upper panel) Root mean squared difference (RMSD) between the daily modeled and satellite-derived SST (OSTIA) time averaged over the model simulation period (1993–2021) separately for **(A)** summer (April–October) and **(B)** winter (November–March) periods. **(C, D)** (Lower panel) Correlation coefficient between the two SST estimates.

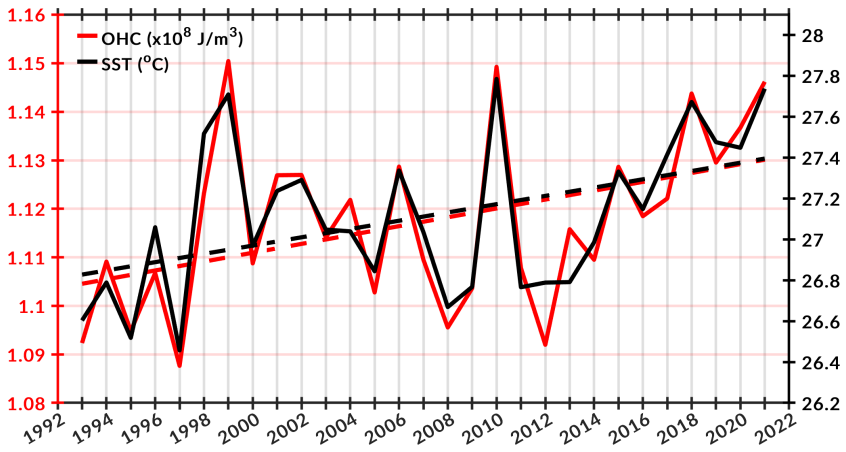

FIGURE 6
Interannual variations of the annual average sea surface temperature (black line) and stored ocean heat content per basin unit volume (red line). The dashed lines represent the linear fitting of the related variations.

the entire simulation period using the following formula:

$$OHC^{t}_{basin} = \sum_{x,y,z} c_p \cdot T_f(x,y,z)\rho_f(x,y,z)\Delta x\Delta y\Delta z \;/\; \sum_{x,y,z} \Delta x\Delta y\Delta z, \quad (1)$$

where c_p is the heat capacity of water (JK^{-1} kg^{-1}), T is the temperature (K), and ρ is the density (kg m^{-3}). In Equation 1, the OHC is normalized by the water volume of the basin because the Gulf is relatively shallow with an average depth of ~35 m and small changes in the sea level can induce considerable alterations to the total basin volume, and thus to the heat content estimation. To remove the effect of sea surface height variability in the temporal evolution of the heat content, the OHC was normalized by the total daily water volume of the basin. Furthermore, the results were averaged over every year (Figure 6, red curve).

OHC demonstrated high interannual variability and a positive statistically significant trend. Due to the shallow nature of the basin, SST is generally a representative of the OHC variability; however, differences appear in several years and even exhibit opposing annual trends (Figure 6, black curve), Nevertheless, the two variables shared a similar long-term trend with a warming rate for OHC of 0.1×10^7 J m^{-3} per decade, indicating that the warming identified in SST in previous studies reflected changes in the entire basin heat content. Peak OHC appeared in the years 1999, 2002, 2006, 2010, 2015, 2018, and 2021 while the lowest value occurred in 1997, coinciding with the high and low SSTs.

3.3 Relative contribution of lateral and surface heat fluxes to heat content change

To evaluate the relative contributions of the advective and surface fluxes to the heat content of the basin, we computed the closed heat budget of the basin. In this case, the heat transported through the SoH, the heat gain/loss due to net surface heat fluxes, and the heat loss due to the water volume that leaves the basin through its surface (as evaporation exceeds precipitation and river runoff) must balance the HCC. The HCC represents the difference of the heat content of the basin between the end and the beginning of each year. Following Tragou et al. (1999), the surface fluxes include the net surface heat forcing, which is the combination of net shortwave radiation (Q_s), latent (Q_h) and sensible heat loss (Q_e), and net longwave emission (Q_b), and they also include the heat loss due to the water loss by evaporation (Q_w).

$$HCS = Q_s + Q_h + Q_e + Q_b + Q_w\,. \quad (2)$$

The last term in Equation 2, Q_w, differs from the latent heat loss and describes the net loss of heat by the water deficit through the surface of the basin (Tragou et al., 1999; Sofianos et al., 2002; Johns et al., 2003; Xue and Eltahir, 2015).

Thus, the heat budget of the basin can be represented as follows:

$$HCC = \Delta H^{t}_{basin} = HCL + HCS, \quad (3)$$

where ΔH^{t}_{basin} is the total heat content difference of the Gulf over the timescale t (a year for the purposes of this work), HCL is the lateral heat content transported through the SoH, and HCS is heat content from the net surface fluxes (heat and freshwater).

The terms in Equation 3 are computed annually from the model daily outputs, following Xue and Eltahir (2015), as below:

$$\Delta H^{t}_{basin} = \sum_{x,y,z} c_p \cdot T_f(x,y,z)\rho_f(x,y,z)\Delta x\Delta y\Delta z - \sum_{x,y,z} c_p \cdot T_i(x,y,z)\rho_i(x,y,z)\Delta x\Delta y\Delta z, \quad (4)$$

$$HCL = \sum_{t}\sum_{y,z} c_p \cdot T(y,z) \cdot \rho(y,z) \cdot u(y,z)\;\; \Delta y\Delta z\Delta t, \quad (5)$$

$$HCS = \sum_{t}\sum_{x,y} [Q_{Net}(x,y) - c_p \cdot T(x,y) \cdot \rho(x,y) \cdot (E(x,y) - P(x,y) - R(x,y))]\Delta x\Delta y\Delta t, \quad (6)$$

where c_p, T, and ρ are the same as in Equation 1; E, P, R, denote evaporation (ms^{-1}), precipitation (ms^{-1}), and river runoff (ms^{-1}),

respectively; u is the meridional velocity through the SoH (ms^{-1}); and Q_{Net} ($W\ m^{-2}$) is the net surface heat flux. The subscripts f and i denote final (last) and initial (first) day for each year. The HCC is further normalized by the total daily volume of the basin to eliminate the impact of sea level variations. Under a closed budget framework, we plot the normalized terms of Equation 3 (Figure 7), as computed by Equations 4–6.

The results for the individual terms of the heat budget are presented in Figure 7. The heat flux attributed to the lateral fluxes (*HCL*; Figure 7, blue color) exhibited relatively moderate interannual variability ranging from 0.68×10^7 to 1.33×10^7 J m^{-3} (equivalent to a range of 6.8–13.8 W m^{-2}), with an increasing trend over time. This indicated that the Gulf gained heat from the open ocean during the entire study period with the maximum heat gain in 2007. The heat transport associated with the net surface fluxes over the Gulf (*HCS*; Figure 7, yellow color) was always negative, resulting in heat loss with strong interannual variations ranging from 0.31×10^7 to 1.69×10^7 J m^{-3} (equivalent to a range of 4.1–17.4 W m^{-2}). Heat loss over the surface presented a decreasing trend over time and was particularly strong in some years with a peak value during 2011 while it was almost zero in 1998.

On average, the contribution by advective and the surface fluxes in the *HCC* of the Gulf is of the same order for the whole period, but the interannual variability of their contribution considerably fluctuated. The relative contribution of lateral fluxes to the *HCC* accounted for over 50% for 17 years, with an average value of $9.22 \pm 1.49 \times 10^6$ J m^{-3} (equivalent to 9.5 ± 1.5 W m^{-2}). The surface fluxes contributed to this change with a similar percentage for the remaining 12 years, with an average value of $9.17 \pm 4.15 \times 10^6$ J m^{-3} (equivalent to 9.4 ± 4.3 W m^{-2}). *HCS* appears to be the factor characterizing *HCC's* interannual variability, while *HCL* is the dominant factor driving its long-term trend.

3.4 Variability and trends of heat transport through the strait of Hormuz

The previously demonstrated long-term variability of the Gulf's heat content is highly impacted by the water exchanges between the Gulf and the open ocean through the SoH (Alsayed et al., 2023). Lateral fluxes play an important role in characterizing the interannual *HCC* of the basin as well as its variability and trend. To that end, we next evaluate the contribution to the heat content of the basin by the heat transported via the SoH, separately considering the role of changes in the transported volumes and their mean temperatures. The heat content transported into (out of) the basin was estimated using Equation 5, considering only the model grid points where the velocity direction is into (out of) the basin. The volume transported by each flow is computed in a similar way, with the heat capacity of water, temperature, and density omitted from Equation 5.

The inflowing heat content (HC_{in}; Figure 8A, red dotted line) shows strong interannual variations with an increasing trend (0.25×10^{19} J yr^{-1}). Similar variability with a relatively smaller positive trend (0.19×10^{19} J yr^{-1}) is evident for the heat transported by the outflowing waters (HC_{out}; Figure 8A, dark orange dotted line). The Gulf experienced a consistent gain of heat through the SoH, while during the entire study period the heat imported through the strait was greater than the one exported. The transport of heat through the SoH was defined by the volume and temperature of the exchanged water mass. The transported volume corresponding to each flow is presented in Figure 8B and it shows a matching pattern in terms of variability and trend with the heat content (Figure 8A), but with slightly higher variability for both flows and similar trends between the outflow and inflow (0.16 and 0.17×10^{11} m^3 yr^{-1}, respectively). Similar to HC_{in} and HC_{out}, the volume of water transported into the Gulf was higher than the outflowing volume

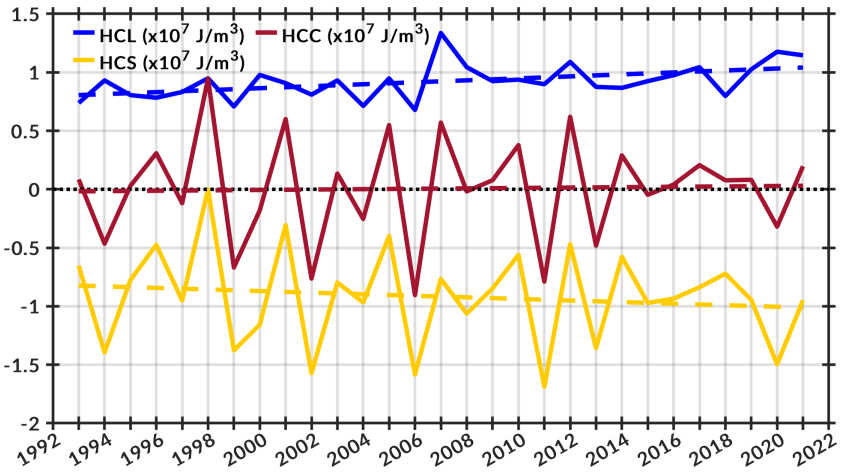

FIGURE 7
Annual values of the heat budget terms per basin unit volume. Positive and negative values indicate heat gain and loss for the basin, respectively. The red color represents the HCC for each year, the blue color represents the heat gain from the lateral exchanges with the open ocean (HCL), and the yellow color represents the heat loss due to net surface fluxes (HCS). The dashed lines represent the linear fitting of related variations.

throughout the simulation period. However, the average temperature of the inflowing/outflowing water volume highly fluctuated interannually and exhibited a positive trend (Figure 8C). For the whole period, the water entering through the SoH (T_{in}; Figure 8C, dark blue line) was warmer, and for some years even much warmer, than the water transported out of the Gulf (T_{out}; Figure 8C, cyan line). Although both flows were getting warmer, the inflow warmed to a considerably higher extent than the outflow with an increasing trend of 0.14°C per decade, which was statistically significant at the 95% confidence level, while the outflow trend was close to zero (0.03°C/decade) and not statistically significant.

These results indicate a clearly upward trend for the transported heat through the SoH, which was driven by positive trends in both the volume of waters exchanged and their temperature. The relative contribution of each factor to the trend of the heat content exchanged through the SoH is estimated (similarly to Xie et al. (2019)) as follows:

$$Tr_{HC_i}^{Vol_i} \cong Tr_{Vol_i}\ \bar{T}_i \cdot c_p\bar{\rho}_i,$$

$$Tr_{HC_i}^{T_i} \cong Tr_{T_i}\ \overline{Vol}_i \cdot c_p\bar{\rho}_i, \tag{7}$$

$$Tr_{HC_i} \cong Tr_{HC_i}^{Vol_i} + Tr_{HC_i}^{T_i},$$

where Vol_i is the volume and T_i is the temperature of the waters exchanged, Tr_{Vol_i} and Tr_{T_i} are the trends of the transported volume of water and of its temperature, Tr_{HC_i} is the total trend of the heat transported through the SoH, while $Tr_{HC_i}^{Vol_i}$ and $Tr_{HC_i}^{T_i}$ represent the partial trends of the transported heat specifically attributed to the volume and temperature of the exchanged waters, respectively. The subscript …$_i$ stands for inflow or outflow and the accent bar …̄ stands for the mean value.

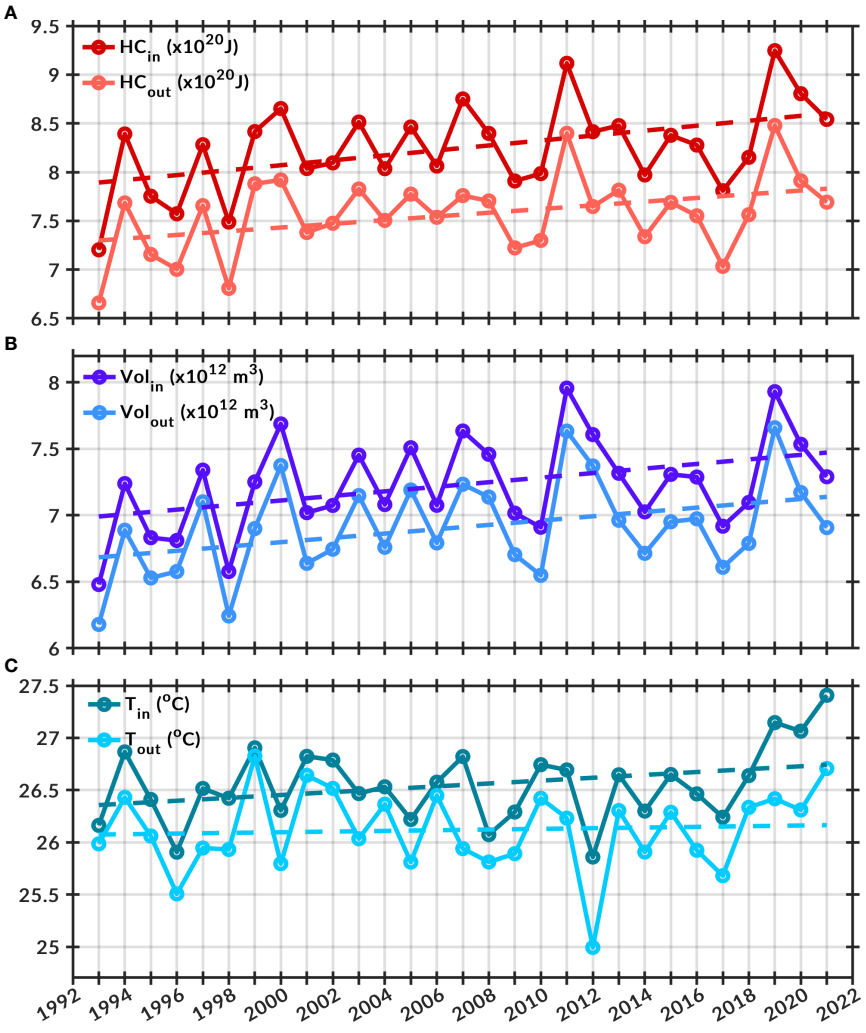

FIGURE 8
Interannual variations of the **(A)** total heat content, **(B)** volume, and **(C)** temperature transported through the Strait of Hormuz. The subscripts in and out for the dotted lines correspond to the results of the inflow and outflow, respectively, with the dashed lines representing the linear fitting of related variations.

denotes the time average of the corresponding variable. Subsequently, each factor's percentage contribution, after Equation 7, can be estimated as ($Tr^{Vol_i}_{HC_i}/Tr_{HC_i}$) · 100 %, and ($Tr^{T_i}_{HC_i}/Tr_{HC_i}$) · 100 %, for volume transport and temperature respectively.

For the $Tr_{HC_{in}}$ ($Tr_{HC_{out}}$), 82% (95%) was attributed to the $Tr^{Vol_{in}}_{HC_{in}}$ ($Tr^{Vol_{out}}_{HC_{out}}$) imposed by the volume of water transported in (out) of the SoH, with the remaining 18% (5%) was attributed to the $Tr^{T_{in}}_{HC_{in}}$ ($Tr^{T_{out}}_{HC_{out}}$) introduced by the trend in the temperature of inflowing (outflowing) water. Accordingly, the dominant factor driving the positive trend in the heat transported through the strait was the increase in the volume of the exchanged waters when compared to the contribution made by the increase in their temperature. Nonetheless, it is important to note that temperature had a significantly greater influence on the heat transported into the Gulf as opposed to its impact on the transported heat out of the basin.

4 Discussion and conclusions

This study investigated the long-term warming response of the Arabian Gulf to local (over the Gulf) and advective (via the exchange of waters with the Indian Ocean through the strait of Hormuz (SoH)) forcing in terms of variability and trends. This was accomplished by analyzing a high-resolution (1/100°) general circulation ocean model simulation covering a 29-year period from 1993 to 2021 that was validated against available satellite-derived data and *in situ* observations. The model results were found to be in close agreement with the observations, suggesting that the model well reproduces the thermohaline structure, the temporal variability of the flow through the SoH, and the overturning circulation of the basin. We examined the trends and long-term fluctuations of the Gulf's sea surface temperature and ocean heat content. Furthermore, we investigated the variability of the heat budget terms and the relative contribution of lateral and surface fluxes on the HCC of the Gulf, focusing on the interannual variations and trends of the transported heat content through the SoH.

Recent studies on the Gulf have revealed significant trends and strong interannual variability with distinct spatial characteristics for the SST (Shirvani et al., 2015; Noori et al., 2019; Hereher, 2020; Mogaddam et al., 2020; Al Senafi, 2022). Over the past 29 years, the average SST of the whole Gulf was estimated to be 27.11°C using our model results and ranged between 26.46°C to 27.79°C, with the coolest year recorded in 1997 and the warmest in 2010. Similar estimates for SST have been reported in recent studies incorporating satellite and observational data (Noori et al., 2019; Al Senafi, 2022). Our results also revealed a considerably increasing warming rate for the basin at 0.2°C per decade. This was close to previous studies that reported a rising trend that changes depending on the region and time period analyzed. For example, Hereher (2020), utilizing remotely sensed SST (MODIS) data for the period 2003–2018 and focusing on specific locations in the Gulf, found an increasing trend ranging from 0.08°C to 0.7°C per decade from east to west. Similar to this study, a positive trend was estimated here at 0.08°C per decade to 0.5°C per decade for the same period. Although SST serves as a crucial indicator for assessing the warming rate of the Gulf and has been extensively utilized in the aforementioned studies, OHC is considered a more appropriate parameter for this evaluation. In this study, the simulated OHC generally exhibited similarities with SST in terms of trend and variability while still showing marked differences in some years. Despite these differences, the results suggest that SST can serve as a representative indicator for the OHC to some extent, and ultimately, for assessing the warming rate of the basin. This highlights the interconnectedness between SST and OHC, emphasizing the importance of considering both parameters in understanding the warming of the Gulf.

To evaluate the parameters that define the change of the heat content and subsequently the Gulf's warming, we analyzed the closed heat budget of the basin. Under such framework, the heat content change must be balanced by the advective heat fluxes through the SoH (HCL) and the net heat fluxes through the surface of the basin (HCS). Both HCL and HCS played a crucial role in shaping the variability and trend of HCC, which strongly fluctuated interannually. The relative contribution of HCL to the HCC was found to account for over 50% over a longer period than that of HCS, and to be the dominant term driving its trend, while HCS was the factor that determined the HCC variability. Alsayed et al. (2023) studied the seasonal variability of the Gulf's OHC over the period 1980–2017 and found that, on average, the annual net heat loss attributed to net surface heat fluxes, which was in agreement with our work. They also suggested that waters exchanged between the Gulf and the open ocean through the SoH may play an important role in increasing the heat content in the southeastern area of the Gulf. In addition, we found that in the long-term, these exchanges drive the increasing rate of heat content of the whole basin.

Furthermore, we emphasized on investigating the heat transported through the SoH, as the lateral fluxes played an important role in defining the interannual basin's HCC, its variability and trend. Our analyses demonstrated a clear increasing trend for the transported heat through the SoH with strong interannual variations that are defined by the trends and variability of the volume transport and its temperature. Considering the inflow and outflow separately, temperature plays a considerably larger role when it comes to the inflowing water heat content trend. However, the dominant factor driving the increase in the exchanged heat content through SoH is found to be the trend in the transported volume rather than the trend in temperature. This was in accordance with a similar study for the neighboring Red Sea (Xie et al., 2019), which revealed that the interannual variability of the exchanges through the strait of Bab-al-Mandeb is primarily controlled by the volume of exchanged waters compared to those by changes in the temperature of the exchanged waters.

The evaporation (which exerts precipitation and river runoff) over the basin drives the flow of relatively fresher water into the Gulf and the outflow of denser higher salinity water by both the overturning and horizontal components of the basin's circulation, which are directly linked to evaporation (Campos et al., 2020). Al-Shehhi et al. (2021) also suggested that this process is the outcome of air–sea fluxes over the Gulf. Herein, we found that the inflow and outflow transports at the SoH, along with the net freshwater fluxes over the Gulf, exhibited increasing trends over the entire simulation

period (not shown). Additionally, our results clearly indicate that the volume transported through the SoH and its mean temperature is increasing. These results suggest that the overturning circulation of the Gulf is accelerating, which appears to be primary driver behind the increase of the heat content of the basin, further augmented by the rise in temperature of the water transported into the basin. The mechanism that drives this acceleration can be either related to the increase of heat loss from the surface (atmospheric component) or the intensification of heat gain through the SoH (inflowing of warmer water), which could lead to stronger fluxes due to the air–sea interaction and the difference between SST and air temperature. To address this, the freshwater budget should be also considered and an extended evaluation of the surface fluxes is required, which we will investigate in our next study.

Previous studies linked Gulf SST trends and anomalies with the El Niño-southern oscillation (ENSO), north Atlantic oscillation, and Atlantic multidecadal oscillation (AMO) (Purkis and Riegl, 2005; Noori et al., 2019; Alawad et al., 2023). High SST anomalies in the Gulf and Gulf of Oman have also been linked to ENSO and the Indian Ocean Zonal Mode during the years 1998, 2002, 2006, and 2010 (Riegl, 2002; Loschnigg et al., 2003; Nandkeolyar et al., 2013). Al Senafi (2022) suggested that ENSO, AMO, and IOD can result in atmospheric changes in the Gulf region, eventually impacting the SST variability. While SST is valuable, the heat content offers distinct advantages in evaluating the warming rate of the Gulf. Throughout the entire period, peak SST and OHC occurred in 1998, 1999, 2002, 2006, 2015, 2018, and 2021 when ENSO events took place with the strongest El Niño events occurring during 1997–1998 and 2015–2016 (Huang et al., 2016; Wang et al., 2017). During ENSO events, the HCS seemed to control the HCC for the period up to 2006 (except 1998), while the HCL dominated in the later years, including 2010, when the warmest year in terms of SST occurred.

Although the relation of SST with climatic modes has been investigated in previous studies, their relation with the heat budget terms (*HCL* and *HCS*), as well as with the heat exchanges through SoH (HC_{in}, HC_{out}, T_{in}, T_{out}) as presented in our study has yet to be examined. This topic along with the mechanism that drives the acceleration of the overturning circulation of the Gulf will be addressed next as part of our ongoing investigation of the regional dynamics and its teleconnections to the global climate variations. Our efforts aim to provide a better understanding of the mechanisms (local vs. remote) driving the warming rate of the basin.

Data availability statement

The original contributions presented in the study are included in the article/Supplementary Material. Further inquiries can be directed to the corresponding author.

Author contributions

PV: Data curation, Methodology, Validation, Visualization, Writing – original draft, Conceptualization, Formal analysis, Investigation. GK: Writing – review & editing, Conceptualization, Methodology, Data curation, Supervision. SL: Writing – review & editing, Conceptualization, Methodology. SS: Writing – review & editing, Conceptualization. IH: Supervision, Writing – review & editing, Conceptualization, Funding acquisition, Project administration.

Funding

The author(s) declare financial support was received for the research, authorship, and/or publication of this article. The reported research was supported by Saudi Aramco and the Office of Sponsored Research (OSR) at King Abdullah University of Science and Technology (KAUST) under the Virtual Red Sea Initiative (Grant #REP/1/3268-01-01).

Acknowledgments

We thank the NOAA National Centers for Environmental Information (NCEI) for providing access to the World Ocean Atlas dataset. OSTIA data were obtained from the Copernicus Marine Environmental Monitoring Service (CMEMS) web portal (http://marine.copernicus.eu/). Model simulations and post-processing of the model outputs were performed on the KAUST supercomputing facility Shaheen-II. We are grateful to KAUST HPC team for their valuable support during the generation and processing the model outputs. We would also like to thank the Reviewers for their insightful comments and constructive suggestions.

Conflict of interest

The authors declare that the research was conducted in the absence of any commercial or financial relationships that could be construed as a potential conflict of interest.

Publisher's note

Supplementary material

The Supplementary Material for this article can be found online at: https://www.frontiersin.org/articles/10.3389/fmars.2023.1260058/full#supplementary-material

References

Abualnaja, Y. O. (2009). Estimation of the net surface heat flux in the Arabian Gulf based on the equilibrium temperature. *J. King Abdulaziz University Mar. Sci.* 20, 21–29. doi: 10.4197/Mar.20-1.2

Adcroft, A., Campin, J.-M., Dutkiewicz, S., Constantinos, E., Ferreira, D., Forget, G., et al. (2017). MITgcm user manual. *Internal Document*. Available at: https://mitgcm-example.readthedocs.io/en/latest/

Ahmad, F., and Sultan, S. A. R. (1991). Annual mean surface heat fluxes in the Arabian gulf and the net heat transport through the strait of hormuz. *Atmosphere - Ocean* 29, 54–61. doi: 10.1080/07055900.1991.9649392

Al Azhar, M., Temimi, M., Zhao, J., and Ghedira, H. (2016). Modeling of circulation in the Arabian Gulf and the Sea of Oman: Skill assessment and seasonal thermohaline structure. *J. Geophys. Res. Oceans* 121, 1700–1720. doi: 10.1002/2015JC011038

Alawad, K. A., Al-Subhi, A. M., Alsaafani, M. A., and Alraddadi, T. M. (2023). What causes the Arabian gulf significant summer sea surface temperature warming trend? *MDPI Journal Atmosphere* 14 (3), 1–12. doi: 10.3390/atmos14030586

Alosairi, Y., and Pokavanich, T. (2017). Seasonal circulation assessments of the Northern Arabian/Persian Gulf. *Mar. pollut. Bull.* 116, 270–290. doi: 10.1016/j.marpolbul.2016.12.065

Alsayed, A. Y., Alsaafani, M. A., Al-Subhi, A. M., Alraddadi, T. M., and Taqi, A. M. (2023). Seasonal variability in ocean heat content and heat flux in the Arabian gulf. *J. Mar. Sci. Eng.* 11, 532. doi: 10.3390/jmse11030532

Al Senafi, F. (2022). Atmosphere-ocean coupled variability in the arabian/persian gulf. *Front. Mar. Sci.* 9. doi: 10.3389/fmars.2022.809355

Al Senafi, F., and Anis, A. (2015). Shamals and climate variability in the Northern Arabian/Persian Gulf from 1973 to 2012. *Int. J. Climatol.* 35, 4509–4528. doi: 10.1002/joc.4302

Al-Shehhi, M. R., Song, H., Scott, J., and Marshall, J. (2021). Water mass transformation and overturning circulation in the Arabian Gulf. *J. Phys. Oceanogr.* 1–42, 3513–3527. doi: 10.1175/JPO-D-20-0249.1

Antonov, J. I., Levitus, S., and Boyer, T. P. (2005). Thermosteric sea level rise 1995-2003. *Geophys. Res. Lett.* 32. doi: 10.1029/2005GL023112

Azam, M. H., Elshorbagy, W., Ichikawa, T., Terasawa, T., and Taguchi, K. (2006). 3D model application to study residual flow in the Arabian gulf. *J. Waterw Port Coast. Ocean Eng.* 132, 388–400. doi: 10.1061/(asce)0733-950x(2006)132:5(388

Bauman, A. G., Feary, D. A., Heron, S. F., Pratchett, M. S., and Burt, J. A. (2013). Multiple environmental factors influence the spatial distribution and structure of reef communities in the northeastern Arabian Peninsula. *Mar. pollut. Bull.* 72, 302–312. doi: 10.1016/j.marpolbul.2012.10.013

Belkin, I. M. (2009). Rapid warming of large marine ecosystems. *Prog. Oceanogr.* 81, 207–213. doi: 10.1016/j.pocean.2009.04.011

Brewer, P. G., and Dyrssen, D. (1985). Chemical oceanography of the Persian gulf. *Prog. Oceanogr.* 14, 41–55. doi: 10.1016/0079-6611(85)90004-7

Brewer, P. G., Fleer, A. P., Kadar, S., and Smith, C. L. (1978). *Report A, chemical oceanographic data from the Persian Gulf and Gulf of Oman* (Woods Hole, MA: Woods Hole Oceanographic Institution). doi: 10.1575/1912/10603

Campos, E. J. D., Gordon, A. L., Kjerfve, B., Vieira, F., and Cavalcante, G. (2020). Freshwater budget in the Persian (Arabian) Gulf and exchanges at the Strait of Hormuz. *PloS One* 15. doi: 10.1371/journal.pone.0233090

Cheng, L., Trenberth, K. E., Fasullo, J., Boyer, T., Abraham, J., and Zhu, J. (2017). Improved estimates of ocean heat content from 1960 to 2015. *Sci. Adv.* 3. doi: 10.1126/sciadv.1601545

Dasari, H. P., Viswanadhapalli, Y., Langodan, S., Abualnaja, Y., Desamsetti, S., Vankayalapati, K., et al. (2022). High-resolution climate characteristics of the Arabian Gulf based on a validated regional reanalysis. *Meteorological Appl.* 29. doi: 10.1002/met.2102

Dee, D. P., Uppala, S. M., and Simmons, A. J. (2011). The ERA-Interim reanalysis: configuration and performance of the data assimilation system - Dee - 2011 - Quarterly Journal of the Royal Meteorological Society - Wiley Online Library. *Q. J. R. Meteorological Soc.* 137 (656), 553–597. doi: 10.1002/qj.828

Donlon, C. J., Martin, M., Stark, J., Roberts-Jones, J., Fiedler, E., and Wimmer, W. (2012). The operational sea surface temperature and sea ice analysis (OSTIA) system. *Remote Sens Environ.* 116, 140–158. doi: 10.1016/j.rse.2010.10.017

Emery, K. O. (1956). Sediments and water of Persian gulf. *Am. Assoc. Pet Geol. Bull.* 40, 2354–2383. doi: 10.1306/5ceae595-16bb-11d7-8645000102c1865d

Garcia-Soto, C., Cheng, L., Caesar, L., Schmidtko, S., Jewett, E. B., Cheripka, A., et al. (2021). An overview of ocean climate change indicators: sea surface temperature, ocean heat content, ocean pH, dissolved oxygen concentration, arctic sea ice extent, thickness and volume, sea level and strength of the AMOC (Atlantic Meridional Overturning Circulation). *Front. Mar. Sci.* 8. doi: 10.3389/FMARS.2021.642372/BIBTEX

Hassanzadeh, S., Hosseinibalam, F., and Rezaei-Latifi, A. (2011). Numerical modelling of salinity variations due to wind and thermohaline forcing in the Persian Gulf. *Appl. Math Model.* 35, 1512–1537. doi: 10.1016/j.apm.2010.09.029

Hastenrath, S., Lamb, P., and Greischar, L. (1979). Climatic atlas of the Indian ocean: the oceanic heat budget. *Univ. Wisconsin Press* 93.

Hereher, M. E. (2020). Assessment of climate change impacts on sea surface temperatures and sea level rise-The Arabian Gulf. *Climate* 8, 1–14. doi: 10.3390/cli8040050

Hosseinibalam, F., Hassanzadeh, S., and Rezaei-Latifi, A. (2011). Three-dimensional numerical modeling of thermohaline and wind-driven circulations in the Persian Gulf. *Appl. Math Model.* 35, 5884–5902. doi: 10.1016/j.apm.2011.05.040

Hoteit, I., Abualnaja, Y., Afzal, S., Ait-El-Fquih, B., Akylas, T., Antony, C., et al. (2021). Towards an end-to-end analysis and prediction system for weather, climate, and Marine applications in the Red Sea. *Bull. Am. Meteorol. Soc.* 102, 99–122. doi: 10.1175/BAMS-D-19-0005.1

Huang, B., L'Heureux, M., Hu, Z. Z., and Zhang, H. M. (2016). Ranking the strongest ENSO events while incorporating SST uncertainty. *Geophys. Res. Lett.* 43, 9165–9172. doi: 10.1002/2016GL070888

Hunter, J. R. (1982). The physical oceanography of the Arabian Gulf: a review and theoretical interpretation of previous observations. in. *First Arabian Gulf Conf. Environ. pollut.*, 1–23.

IPCC (2019) *Special report: the ocean and cryosphere in a changing climate*. Available at: https://www.ipcc.ch/report/srocc/.

John, V., Coles, S., and Abozed, A. (1990). Seasonal cycles of temperature, salinity and water masses of the Western Arabian Gulf. *Oceanologica Acta* 13, 273–282.

Johns, W. E., Yao, F., Olson, D. B., Josey, S. A., Grist, J. P., and Smeed, D. A. (2003). Observations of seasonal exchange through the Straits of Hormuz and the inferred heat and freshwater budgets of the Persian Gulf. *J. Geophysical Res. C: Oceans* 108, 21–21. doi: 10.1029/2003jc001881

Kämpf, J., and Sadrinasab, M. (2006). The circulation of the Persian Gulf: a numerical study. *Ocean Sci.* 2, 27–41. doi: 10.5194/os-2-27-2006

Krokos, G., Papadopoulos, V. P., Sofianos, S. S., Ombao, H., Dybczak, P., and Hoteit, I. (2019). Natural climate oscillations may counteract red sea warming over the coming decades. *Geophys. Res. Lett.* 46, 3454–3461. doi: 10.1029/2018GL081397

Langodan, S., Cavaleri, L., Vishwanadhapalli, Y., Pomaro, A., Bertotti, L., and Hoteit, I. (2017). The climatology of the Red Sea – part 1: the wind. *Int. J. Climatol.* 37, 4509–4517. doi: 10.1002/joc.5103

Large, W. G., McWilliams, J. C., and Doney, S. C. (1994). Oceanic vertical mixing: A review and a model with a nonlocal boundary layer parameterization. *Rev. Geophys.* 32, 363–403. doi: 10.1029/94RG01872

Large, W. G., and Pond, S. (1981). Open ocean momentum flux measurements in moderate to strong winds. *J. Phys. OCEANOGR.* 11, 324–336. doi: 10.1175/1520-0485(1981)011<0324:oomfmi>2.0.co;2

Large, W. G., and Yeager, S. G. (2012). On the observed trends and changes in global sea surface temperature and air-sea heat fluxes (1984-2006). *J. Clim* 25, 6123–6135. doi: 10.1175/JCLI-D-11-00148.1

Layeghi, B. A., Bidokhti, A. A., Ghader, S., and Azadi, M. (2019). Numerical simulations of oceanographic characteristics of the Persian Gulf and Sea of Oman using ROMS model. *Indian J. Geo-Marine Sci.* 48, 1978–1989. doi: 10.30467/NIVAR.2019.91474

Levitus, S., Antonov, J. I., Boyer, T. P., and Stephens, C. (2000). Warming of the world ocean. *Sci. (1979)* 287, 2225–2229. doi: 10.1126/science.287.5461.2225

Lorenz, M., Klingbeil, K., and Burchard, H. (2020). Numerical study of the exchange flow of the Persian gulf using an extended total exchange flow analysis framework. *J. Geophys. Res. Oceans* 125. doi: 10.1029/2019jc015527

Loschnigg, J., Meehl, G. A., Webster, P. J., Arblaster, J. M., and Compo, G. P. (2003). The Asian Monsoon, the tropospheric biennial oscillation, and the Indian Ocean zonal mode in the NCAR CSM. *J. Clim* 16, 1617–1642. doi: 10.1175/1520-0442(2003)016<1617:TAMTTB>2.0.CO;2

Marshall, J., Adcroft, A., Hill, C., Perelman, L., and Heisey, C. (1997). A finite-volume, incompressible Navier Stokes model for studies of the ocean on parallel computers. *J. Geophys. Res.* 102, 5753–5766. doi: 10.1029/96JC02775

Meshal, A. H., and Hassan, H. M. (1986). Evaporation from the coastal water of the central part of the Gulf. *Arab Gulf J. Scient. Res.* 4, 649–655.

Meyssignac, B., Boyer, T., Zhao, Z., Hakuba, M. Z., Landerer, F. W., Stammer, D., et al. (2019). Measuring global ocean heat content to estimate the earth energy imbalance. *Front. Mar. Sci.* 6. doi: 10.3389/fmars.2019.00432

Michael Reynolds, R. (1993). Physical oceanography of the Gulf, Strait of Hormuz, and the Gulf of Oman-Results from the Mt Mitchell expedition. *Mar. pollut. Bull.* 27, 35–59. doi: 10.1016/0025-326X(93)90007-7

Mogaddam, S. F., Bidokhti, A. A., Givi, F. A., and Ezam, M. (2020). Evaluation of physical changes (temperature and salinity) in the Persian Gulf waters due to climate change using field data and numerical modeling. *Int. J. Environ. Sci. Technol.* 17, 2141–2152. doi: 10.1007/s13762-019-02532-y

Nagamani, P. V., Ali, M. M., Goni, G. J., Udaya Bhaskar, T. V. S., Mccreary, J. P., Weller, R. A., et al. (2016). Heat content of the Arabian Sea Mini Warm Pool is increasing. *Atmospheric Sci. Lett.* 17, 39–42. doi: 10.1002/asl.596

Nandkeolyar, N., Raman, M., Kiran, G. S., and Ajai, (2013). Comparative analysis of sea surface temperature pattern in the Eastern and Western gulfs of Arabian sea and the red sea in recent past using satellite data. *Int. J. Oceanogr.* 2013 doi: 10.1155/2013/501602

Nath, S., Kotal, S. D., and Kundu, P. K. (2016). Decadal variation of ocean heat content and tropical cyclone activity over the Bay of Bengal. *J. Earth System Sci.* 125, 65–74. doi: 10.1007/s12040-015-0651-0

Noori, R., Tian, F., Berndtsson, R., Abbasi, M. R., Naseh, M. V., Modabberi, A., et al. (2019). Recent and future trends in sea surface temperature across the persian gulf and gulf of Oman. *PloS One* 14, 1–19. doi: 10.1371/journal.pone.0212790

Pisano, A., Marullo, S., Artale, V., Falcini, F., Yang, C., Leonelli, F. E., et al. (2020). New evidence of Mediterranean climate change and variability from Sea Surface Temperature observations. *Remote Sens (Basel)* 12. doi: 10.3390/RS12010132

Pous, S., Carton, X., and Lazure, P. (2013a). A process study of the tidal circulation in the Persian gulf. *Open J. Mar. Sci.* 03, 1–11. doi: 10.4236/ojms.2013.31001

Pous, S., Carton, X., and Lazure, P. (2013b). A process study of the wind-induced circulation in the Persian gulf. *Open J. Mar. Sci.* 03, 1–11. doi: 10.4236/ojms.2013.31001

Pous, S., Lazure, P., and Carton, X. (2015). A model of the general circulation in the Persian Gulf and in the Strait of Hormuz: Intraseasonal to interannual variability. *Cont Shelf Res.* 94, 55–70. doi: 10.1016/j.csr.2014.12.008

Prasad, T. G., Ikeda, M., and Kumar, S. P. (2001). Seasonal spreading of the Persian Gulf Water mass in the Arabian Sea. *J. Geophys. Res. Oceans* 106, 17059–17071. doi: 10.1029/2000jc000480

Privett, D. W. (1959). Monthly charts of evaporation from the N. Indian Ocean (including the Red Sea and the Persian Gulf). *Q. J. R. Meteorological Soc.* 85, 424–428. doi: 10.1002/qj.49708536614

Purkis, S. J., and Riegl, B. (2005). Spatial and temporal dynamics of Arabian Gulf coral assemblages quantified from remote-sensing and in *situ* monitoring data. *Mar. Ecol. Prog. Ser.* 287, 99–113. doi: 10.3354/meps287099

Reid, P. C., and Beaugrand, G. G. (2012). Global synchrony of an accelerating rise in sea surface temperature. *J. Mar. Biol. Assoc. United Kingdom* 92, 1435–1450. doi: 10.1017/S0025315412000549

Riegl, B. (2002). Effects of the 1996 and 1998 positive sea-surface temperature anomalies on corals, coral diseases and fish in the Arabian Gulf (Dubai, UAE). *Mar. Biol.* 140, 29–40. doi: 10.1007/s002270100676

Ross, D. A., and Stoffers, P. (1978). Report C, general data on bottom sediments including concentration of various elements and hydrocarbons in the Persian Gulf and Gulf of Oman. Report D, general data on the geophysical nature of the Persian Gulf and Gulf of Oman. *Woods Hole Oceanogr. Inst., Woods Hole, Mass*. Tech. Rep. WHOI-78-39, 107 pp. doi: 10.1575/1912/10604

Sadrinasab, M., and Kämpf, J. (2004). Three-dimensional flushing times of the Persian Gulf. *Geophys. Res. Lett.* 31, 1–4. doi: 10.1029/2004GL020425

Shenn-Yu, C., Kao, T. W., and Al-Hajri, K. R. (1992). A numerical investigation of circulation in the Arabian Gulf. *J. Geophys. Res.* 97, 11219–11236. doi: 10.1029/92jc00841

Shirvani, A., Nazemosadat, S. M. J., and Kahya, E. (2015). Analyses of the Persian Gulf sea surface temperature: prediction and detection of climate change signals. *Arabian J. Geosciences* 8, 2121–2130. doi: 10.1007/s12517-014-1278-1

Sofianos, S. S., Johns, W. E., and Murray, S. P. (2002). Heat and freshwater budgets in the Red Sea from direct observations at Bab el Mandeb. *Deep Sea Res. 2 Top. Stud. Oceanogr.* 49, 1323–1340. doi: 10.1016/S0967-0645(01)00164-3

Storto, A., Masina, S., Simoncelli, S., Iovino, D., Cipollone, A., Drevillon, M., et al. (2019). The added value of the multi-system spread information for ocean heat content and steric sea level investigations in the CMEMS GREP ensemble reanalysis product. *Clim Dyn* 53, 287–312. doi: 10.1007/s00382-018-4585-5

Swift, S. A., and Bower, A. S. (2003). Formation and circulation of dense water in the Persian/Arabian Gulf. *J. Geophysical Res. C: Oceans* 108, 4–1. doi: 10.1029/2002jc001360

Thoppil, P. G., and Hogan, P. J. (2009). On the mechanisms of episodic salinity outflow events in the strait of hormuz. *J. Phys. Oceanogr.* 39, 1340–1360. doi: 10.1175/2008JPO3941.1

Thoppil, P. G., and Hogan, P. J. (2010a). A modeling study of circulation and eddies in the persian gulf. *J. Phys. Oceanogr.* 40, 2122–2134. doi: 10.1175/2010JPO4227.1

Thoppil, P. G., and Hogan, P. J. (2010b). Persian Gulf response to a wintertime shamal wind event. *Deep Sea Res. 1 Oceanogr. Res. Pap* 57, 946–955. doi: 10.1016/j.dsr.2010.03.002

Ting, M., Kushnir, Y., Seager, R., and Li, C. (2009). Forced and internal twentieth-century SST trends in the North Atlantic. *J. Clim* 22, 1469–1481. doi: 10.1175/2008JCLI2561.1

Tragou, E., Garrett, C., Outerbridge, R., and Gilman, C. (1999). The heat and freshwater budgets of the Red Sea. *J. Phys. Oceanogr.* 29, 2504–2522. doi: 10.1175/1520-0485(1999)029<2504:THAFBO>2.0.CO;2

Vasou, P., Vervatis, V., Krokos, G., Hoteit, I., and Sofianos, S. (2020). Variability of water exchanges through the Strait of Hormuz. *Ocean Dyn* 70, 1053–1065. doi: 10.1007/s10236-020-01384-2

Vaughan, G. O., and Burt, J. A. (2016). The changing dynamics of coral reef science in Arabia. *Mar. pollut. Bull.* 105, 441–458. doi: 10.1016/j.marpolbul.2015.10.052

Viswanadhapalli, Y., Dasari, H. P., Langodan, S., Challa, V. S., and Hoteit, I. (2017). Climatic features of the Red Sea from a regional assimilative model. *Int. J. Climatol.* 37, 2563–2581. doi: 10.1002/joc.4865

Wang, B., Li, J., and He, Q. (2017). Variable and robust East Asian monsoon rainfall response to El Niño over the past 60 years, (1957–2016). *Adv. Atmos Sci.* 34, 1235–1248. doi: 10.1007/s00376-017-7016-3

Willis, J. K., Roemmich, D., and Cornuelle, B. (2004). Interannual variability in upper ocean heat content, temperature, and thermosteric expansion on global scales. *J. Geophys. Res. Oceans* 109. doi: 10.1029/2003JC002260

Xie, J., Krokos, G., Sofianos, S., and Hoteit, I. (2019). Interannual variability of the exchange flow through the strait of bab-al-mandeb. *J. Geophys. Res. Oceans* 124, 1988–2009. doi: 10.1029/2018JC014478

Xue, P., and Eltahir, E. A. B. (2015). Estimation of the heat and water budgets of the Persian (Arabian) gulf using a regional climate model. *J. Clim* 28, 5041–5062. doi: 10.1175/JCLI-D-14-00189.1

Yao, F., and Johns, W. E. (2010a). A HYCOM modeling study of the Persian Gulf: 1. Model configurations and surface circulation. *J. Geophys. Res. Oceans* 115. doi: 10.1029/2009JC005781

Yao, F., and Johns, W. E. (2010b). A HYCOM modeling study of the Persian Gulf: 2. Formation and export of Persian Gulf Water. *J. Geophys. Res. Oceans* 115. doi: 10.1029/2009JC005788